

Physico-Mechanical Properties and Microstructure of Blended Cement Incorporating Nano-Silica

Saleh Abd El-Aleem Mohamed

Ass. Prof., Chemistry Department Faculty of Science,
Fayoum University Fayoum-

Abd El-Rahman Ragab

Quality Department, Lafarge Cement El Kattamia, El
Sokhna Suez-

Abstract-In the recent years, the application of nanotechnology in the field of construction and building materials has exponentially increased to produce new materials with novel function and better performance at unprecedented levels. Actually, nano-materials (NMs) can change the concrete world, due to their unique properties, which different from those of the conventional materials. NMs were used either to replace part of cement, producing ecological profile concrete or as admixtures in cement pastes. One of the most commonly used NMs is nano-silica (NS). In this study, the physico-mechanical properties of Portland cement (Type 1) containing NS up to 6.0 mass, % was studied with curing time up to 90-days. The results show that, NS increases the water of consistency as well as setting times, due to its higher specific surface area than OPC. The results of chemically combined water (W_n), free lime (FL), bulk density (BD), and compressive strength (CS) prove that, NS up to 2.0-4.0, mass % seems to be an effective substituent for blending with OPC to improve its physico-mechanical properties. This mainly due to that; NS-particles behave not only as nano-fillers to improve the microstructure of cement paste, but also as activators to promote the hydration of cement phases. The formation of more amounts of CSH in presence of NS was confirmed by XRD and SEM techniques. At higher substitution of OPC with NS (>4.0 mass, %), the values of BD and CS are reduced but still higher than those of the control sample. OPC could be advantageously replaced by 2.0-4.0 mass, % NS, which is the most effective level of NS for producing high-performance blended cement mortars.

Key Words: Portland blended cement, Nano-silica, Physico-mechanical characteristics and Microstructure.

I. INTRODUCTION

Nanotechnology (NT) has become an important key in the field of construction and building materials. NT can be considered as the most modern aspect in every domain of science and technology [1, 2]. For construction sector, NT can be defined as science of controlling the properties at nanometer scale, which can make revolutionary changes in bulk material properties. Nowadays, the micro-level does not provide enough insights into construction and building materials. Therefore, all over the world, increasing amounts of

funding are being directed to research projects dealing with material properties on the nano-level, which is claimed to have a tremendous potential for the future [3]. The evolution of NT provides materials with new properties and over the last years a lot of effort has been put to introduce nano-materials (NMs) into cement pastes, mortars and concretes in order to improve their properties and produce new materials with novel functions as well as better performance at unprecedented levels [4]. Actually, NMs can change the concrete world, due to their unique physical and chemical properties, which different from those of the conventional materials [5]. Nano-materials were used either to replace part of cement, producing ecological profile concrete or as admixtures in cement pastes [6]. In both cases, the addition of them improves the performance of cement paste; in the fresh and hardened states [7]. Different types of NMs have been used in concrete mixtures in order to improve both the mechanical properties and pore structure of the concrete. When using NMs, three main advantages are considered: i) Production of high strength concrete (HSC) for specific applications, ii) Reduction of cement consumption for specific grade of concrete, and iii) The reduction of the construction period, because NMs can produce HSC at short curing times [4]. Due to the longer service life of HSC and its use, which reduces repair and maintenance structure costs. These advantages will help in decreasing the national energy consumption, the overall cost of the structure, and the environmental pollution to a great extent [8, 9]. The great reactivity of NMs is attributed to their high purity and large specific surface area in relation to their volume. In this way, nano-particles (NPs) with 4 nm diameter have more than 50.0 % of its atoms at the surface and are thus very reactive [10]. Due to their sizes, some researchers have recorded an increased water demand for mixtures containing NMs of the same workability [11]. Also, their tendency to agglomerate can be restricted by using dispersing admixtures or by applying different techniques during mixing process [12]. The fundamental processes that govern the concrete properties are affected by the performance of the material on nano-scale. The main hydration product of cement-based materials, the CSH gel,

is a nano-structured material [13]. The nano-scale observations revealed that, the nano-crystallized CSH and also nano-particles (NPs) have been found to act as nuclei for cement phases, promoting their hydration rates [14]. The mechanical properties of concrete mainly depend on the refinement of the microstructure of the hardened cement paste and the improvement of the paste aggregate interfacial transition zone (ITZ) [2]. The role of NPs can be summarized as follow: i) NPs act as fillers in the empty spaces; ii) well dispersed NPs act as crystallization centers of hydrated products, increasing hydration rates of cement phases, iii) NPs assist towards the formation of small sized CH crystals as well as homogeneous clusters of C-S-H, and iv) NPs improve the structure of the ITZ [5, 9]. The most common used NMs in cement pastes, mortars and concretes are nano-sized SiO₂ (NS), TiO₂ (NT), Al₂O₃ (NA), Fe₂O₃ (NF), ZnO₂ (NZ), and carbon nano-tubes (CNT) [15, 16]. Among of them, NS has a significant role to increase the compressive strength and to reduce the overall permeability of hardened concrete. This is attributed to the pozzolanic reaction of the amorphous NS with the liberated portlandite during the hydration of cement, which is resulting in the formation of finer hydrated phases (CSH gel), densified microstructure (nano-filler and anti-leaching effects) and enhanced mechanical properties [17-25]. Accelerated hydration of cement paste and faster formation of CH at initial period was observed in the nano-modified cement paste. This due to the high surface area of NS and thus high reaction rate. NS-particles act as nucleation sites to accelerate the hydration of cement phases [26, 27]. Shih et al. [28] studied the influence of NS on characterization of Portland cement composite and concluded that, the optimal mix proportion is the set of cement: water: NS=1: 0.55: 0.06, which has the highest compressive strength of 65.62 MPa at hydration age of 56-days. By comparison with the control set, the ratio of maximum increase in compressive strength is about 60.6 % at age of 14-days and reduces to 43.8 % at 56-days. Li et al. [5] have been investigated the properties of cement mortars with different NPs to explore their super-mechanical properties. It has been accepted that, NS particles not only are environment-friendly but also could lead to better physio-mechanical properties. In addition, NS helps to save the amount of cement, reduce the mixing water, improve the permeability, decrease the final cost of work, and lower the environmental contaminations. As a consequence of its size, NS-concrete can generate nano-crystals of CSH that can fill up all the micro and nano-

II. MATERIALS AND EXPERIMENTAL TECHNIQUES

A. Materials

The starting materials used in this study were the ASTM Type (I) ordinary Portland cement (OPC) and nano-silica (NS). OPC with Blain surface area of 3000±50 cm²/g was provided from Lafarge Cement Company, Egypt. Its chemical analysis is given in Table 1. Also, its mineralogical composition is listed in Table 2. Nano-silica (NS) with average particle size, Blain surface area and purity percentage of about 15 nm, 50 m²/g and 99.9 %

pores, which were left unfilled in the traditional, cement based concrete. Givi et al. [29] reported that, NS-blended concrete has higher compressive, flexural and tensile strengths at all hydration ages in comparison to control concrete. Also, it has been found that, the cement could be advantageously replaced by NS up to 2.0 mass, % with average particle size of 15 and 80 nm. From the free energy point of view, it can be concluded that, NS with average diameter of 15.0 nm can improve the early age strength of the concrete more than that with 80.0 nm. Babu [30] studied the effect of NS on properties of blended cement. The rate of pozzolanic reaction of NS with the liberated lime during cement hydration is proportional to the surface area available for reaction. The results indicated that, the setting times were elongated with the NS content up to 3.0 mass, %. Also, the pozzolanic reactivity of NS was much higher and quicker up to 3.0 %. However, when the NS content increased from 3.0-6.0 mass, % it did not show any improvement in CH consumption [31]. In previous works [32-34], the addition of NS improved the hydration characteristics and modified the microstructure as well as porosity of cement paste and increased the average chain length of silicates. By consumption of calcium, NS helps in reduction of calcium leaching rate. Singh et al. [35] has reported that, the CH content in NS-cement paste reduced by 86.0 % at 1-day and up to 62.0% at 28-days of hydration. Stefanidou et al. [36] studied the influence of NS on the properties of Portland cement with curing time and reported that, NS appears to affect the mechanical properties and structure of cement pastes even in low concentrations. In this case, 0.5 up to 2.0 mass, % NS instead of cement can cause 20-25% strength increase despite the increased demand in mixing water from 30.0 to 35.0 %. Impressive changes were also recorded in the structure of nano-modified samples as the CSH crystal size is larger in samples with high NS content. This is obvious in pastes with 5.0 mass, % NS where crystals of 1.20 μm average size were formed at 14-days of hydration, while at the same age in pastes with 1.0 mass,% NS, the average crystal size of CSH was 600.0 nm. This work aims to study the physico-mechanical properties and microstructure of Portland blended cements prepared from substitution of different percentages of OPC by NS up to 6.0 mass, %. The water of consistency, initial and final setting times were determined for each cement paste. Also, the values of combined water, free lime, bulk density and compressive strength of hardened cement specimens were measured as a function of curing time up to 90-days.

respectively was supplied from nanotechnology Lab, Faculty of Science, Beni-Suef University, Beni-Suef, Egypt.

B. Experimental techniques

Nano-silica was prepared as follow: In a typical procedure, a desired amount of Na₂SiO₃ solution was diluted with distilled water; the solution stirred for 15 min, and then precipitated using diluted hydrochloric acid. The precipitate was filtered and washed several times with distilled water till free from chloride, and then the

precipitate was dried overnight. To decrease the particle size of the prepared powder, it was milled using ball mill (600 rpm) for 10 hours. The amorphous nature of NS-particles was verified using XRD, SEM and TEM techniques (Figs.1, 2 and 3). OPC was partially substituted with NS up to 6.0 mass, %. Each dry mix was blended in a steel ball mill using five balls for 1 hour in order to attain complete homogeneity. The cement blends were mixed in a rotary mixer. NS-particles are not easy to disperse uniformly in water, due to their high surface energy. Accordingly, the mixing was performed as follows: a) NS was stirred with 25.0 % of the required water for standard consistency at high speed of 120 rpm for 2 min., b) The cement and the residual amount of mixing water were added to the mixer and homogenized at medium speed (80 rpm) for another 2 min., c) The mixture was allowed to rest for 90 second, and then mixed for 1 min at high speed (120 rpm) and d) The paste was manually placed, pressed and homogenized in stainless steel moulds. After the top layer was compacted, the top surface of the mould was smoothed by the aid of thin edged trowel. For preparation of mortars, the sand was added gradually in step b) and mixed at medium speed for additional 30 second. The mortars were prepared according to ASTM (C109-93) by mixing 1 part of cement and 2.75 parts of Lafarge standard sand proportion by weighing with water content sufficient to obtain a flow of 110 ± 5 with 25 drops of the flowing table [37]. Freshly prepared cement mortars were placed in $50 \times 50 \times 50$ mm cubic moulds into two approximately equal layers manually compacted and pressed until a homogeneous specimen was obtained. The moulds were vibrated for a few minutes to remove any air bubbles and to give a better compaction. The mix composition of different cement blends is given in Table 3. The required water of standard consistency gives a paste which permitted the settlement of the Vicat plunger (10 mm in diameter) to a point 5-7 mm from the bottom of the Vicat moulds. It was measured to get all specimens having the same workability. The required water of standard consistency and setting times for each mix were determined according to ASTM specification [38]. The specimens were cured in a humidifier (100% R.H) at room temperature 23 ± 2 °C for 24 hours, then immersed in tap water until the time of testing (Fig. 4). After the predetermined curing time, the hydration of cement pastes was stopped by pulverizing 10 grams of representative sample in a beaker containing methanol-acetone mixture (1:1), and then mechanically stirred for 1 h. The mixture was filtered through a gouch crucible, G4 and washed several times with the stopping solution then with ether. The solid was dried at 70°C for 1 hour to complete evaporation of alcohol, then collected in polyethylene bags; sealed and stored in desiccators for analysis [39]. The chemically combined water content (W_n , %) is used as an indication for the degree of cement hydration. W_n is that portion retained in the sample after the free water is removed. The W_n , % is considered as the

III. RESULTS AND DISCUSSION

A. Water of standard consistency and setting times

percent of ignition loss of the dried sample (on the ignited weight basis). Approximately 2 grams of the pre-dried sample were ignited at 1000°C for 1 hour. The results of W_n , % were corrected for the water of free lime present in each sample [40]. The free lime content of each hydrated cement paste was estimated by the following method, the sample (0.5 g) was poured in 40 ml of a glycerol-ethanol mixture (1:5 v/v), together with a small amount of anhydrous $BaCl_2$ (0.5g) as a catalyst, and phenolphthalein as an indicator. This mixture was kept in a conical flask, fitted with an air reflux, heated on a hot plate for 30 minutes (the color becomes pink). The contents of the flask were titrated with a standardized alcoholic ammonium acetate solution until the pink color just disappeared. Heating was again affected, and if the pink color reappears, the titration was completed with ammonium acetate solution until no further appearance of pink color occurs up on heating [41]. CaO , % = $[(W_1 \times V) / W] \times 100$, W = original weight, W_1 = weight of CaO equivalent to amount of added alcoholic ammonium acetate, V = volume of ammonium acetate per ml. The bulk density (BD) was carried out on cement pastes. Samples were suspended weighed in water and in air (saturated surface dry). Each measurement was conducted on at least three similar cubes of the same mix composition and curing time. Then, the density was calculated as described elsewhere [42]. Compressive strength was determined according to ASTM (C-150) [43], a set of three cubes was tested on a compressive strength machine (3R), Germany, with maximum capacity of 150 MPa force (Fig. 5). To verify the mechanism predicted by the chemical and mechanical tests, some selected hydration products were investigated using XRD, DSC, TG and SEM techniques. The powder method of XRD was adopted in the present study. For this, a Philips diffractometer PW 1730.0 with X-ray source of $Cu \text{ } \alpha$ radiation ($\lambda = 1.5418 \text{ \AA}$) was used (Fig. 6). The scan step size was 2 θ . The collection time 1s, and in the range of 2 θ from 10.0° to 55.0°. The X-ray tube voltage and current were fixed at 40.0 KV and 40.0 mA respectively. An on-line search of a standard database (JCPDS database) for X-ray powder diffraction pattern enables phase identification for a large variety of crystalline phases in a sample. For scanning electron microscopic investigation, SEM, model quanta 250.0 FEG (Field Emission Gun) was used, with accelerating voltage 30.0 K.V., with magnification power 14 x up to 1000000 and resolution for Gun.1n). FEI Company, Netherlands (Fig. 7). The DTA was carried out in air using a DT-30 Thermal Analyzer Shimadzu Co., koyoto, Japan (Fig.8). Calcined alumina was used as inert material, about 50 mg (-76 μ m) of each. The finely ground hydrated cement paste were housed in a small platinum-rhodium crucible. A uniform heating rate was adopted in all of the experiments at 20°C/min [44].

Figures (9&10) show respectively the variations of water of consistency (w/c, %) and setting times of the investigated cement pastes with NS, %. The results show

that, the values of w/c, % increase with NS percentage up to 6.0 mass,%, which is mainly attributed to the increase of surface area and decrease of crystal lattice [45-47]. Thus, the specimens containing NS require more water to rapid forming of hydrated products [20]. The initial and final setting times (IST&FST) are elongated by replacement of OPC with 2.0 mass,% NS. This is due to the high water of consistency. As the NS content increases up to 4.0 mass, %, and the setting times are shortened, due to the formation of excessive amount of CSH, which fill up some of open pores originally filled with water that accelerates the setting. But, at 6.0 mass,% NS, the setting times are elongated, due to either the increase of water of consistency or the coating effect of NS particles on the cement grains, then the setting is retarded [6].

B. Chemically combined water contents (Wn, %)

The variation of Wn %, of hydrated OPC and NS-blended cement pastes as a function of NS content are graphically represented in Fig. (11). It is apparent that, Wn, %, increases with curing time for all hydrated cement pastes. This mainly due to the continuous hydration of cement phases as well as NS-pozzolanic reaction, leading to the formation of more hydrated products. It is obvious that, the values of Wn increase with the NS % from 2.0 to 6.0 mass, % with two different rates. The first (from 2.0 to 4.0%) is faster than the second (>4.0-6.0%). At 4.0% NS, the combined water content decreases, but still more than that of the control sample OPC. The increase of Wn, % with NS content is mainly due to two factors work together, the first is the high-water demand and the second is the Pozzolanic reactivity of NS. Nano-silica reacts with the liberated CH during cement hydration, leading to the formation of additional hydrated products such as CSH, which increases the combined water content. The results also show that, NS accelerates the hydration of cement phases, especially at early ages of hydration (0-28 days) [51]. It is clear that, 4.0% NS gives higher Wn contents than OPC and with 6% NS. This result is in agreement with the values of setting times.

C. Free lime contents (F.L, %)

The Pozzolanic reaction rate of NS with the liberated $\text{Ca}(\text{OH})_2$ during cement hydration can be followed by monitoring the decrease in F.L,% with curing time and NS,%. The free lime, % of hydrated OPC and NS-cement pastes up to 90-days are graphically plotted in Fig.(12). The results show that, the F.L values of OPC paste increases with curing time. On the other side, the presence of NS tends to decrease the residual Protlandite (CH), due to the Pozzolanic reaction between the amorphous glassy NS and free CH liberated from calcium silicate hydration [21]. It is clear that, the cement paste with 4% NS gives the lower F.L contents than OPC with 6 % NS. This result is also in agreement with that of combined water. It can be said that, 4% is the optimum replacement level of OPC with NS. At high NS content (6%), the NS-particles coat the hydrated products and consequently retard the hydration reaction as well as the mechanical properties.

D. Bulk density (BD)

Fig. (13) shows the values of BD of OPC and NS-cement pastes hydrated up to 90-days. It is clear that, BD increases with curing time for all hydrated cement pastes, due to the continuous hydration of cement phases, leading to the formation and accumulation of excessive amounts of denser products (CSH, CAH and CASH), which tend to increase the gel/space ratio as well as the bulk density [39, 48]. The bulk density increases with NS, % up to 4%, then decreases at 6%. This can be interpreted as follows [20]: Suppose that, NS particles are uniformly dispersed in cement paste, after the hydration begins, hydrated products diffuse and envelop the NPs as kernels. If the NS content and the distance between them are appropriate, the crystallization will be controlled to be a suitable state through restricting the growth of CH crystals. Moreover, the NPs located in cement paste as kernels can further promote cement hydration, due to their high reactivity. This makes the size of CH crystals smaller, the cement matrix is more homogeneous and compact. Consequently, the pore structure is improved. With increasing NS content more than 4%, the improvement of the pore structure of cement paste is weakened. This may be due to that, the distance between NPs decreases with NS content and CH crystals can not grow up enough due to limited space, then the crystal quantity is decreased, leading to the decrease of crystal to strengthening gel ratio [47].

E. Compressive strength

The effect of NS content on the compressive strength (CS) of the hydrated OPC and blended cement mortars up to 90-days is shown in Fig.(14). It can be seen that, the values of CS increase with curing time for all hydrated cement mortars, due to the continuous hydration and formation of successive amounts of hydrated silicates, which is the main source of strength. These products accumulate in water filled pores to form a more compact structure [48]. Also, the compressive strength of the investigated cement mortars increases sharply with NS % up to 4.0% then decreases but still more than that of the plain cement mortar up to 28-days. The improvement of compressive strength in the presence of NS up to 4.0% is due to that; NS behaves not only as a filler to improve microstructure, but also as an activator to promote pozzolanic reaction. Both the nucleation and pozzolanic effects of NS lead to more accumulation of hydration products, leading to the formation of homogeneous, denser and compact microstructure. Consequently the bulk density (BD) and compressive strength (CS) increase with NS up to 4.0%. The decrease of compressive strength at 6.0% NS is due to the decrease of bulk density [49].

F. XRD analysis

XRD patterns of hydrated M2 (96.0% OPC+4.0% NS) as a function of curing time are shown in Fig. (15). The results indicate that, the intensities of CSH and CC peaks increase with curing time up to 90-days. But, the peaks corresponding to CH and anhydrous silicates behave in opposite manner, i.e. decrease with time, due to the continuous hydration of cement clinker phases as well as

the pozzolanic reaction of NS with the liberated CH during cement hydration, leading to more portlandite consumption and CSH formation. The effect of NS on the hydration rate of OPC can be seen from Figs. (16-19), which represent the XRD patterns of M0 and NS-blended cement pastes hydrated at the same age. It is obvious that, NS affects positively the hydration of cement phases, due to its nano-size and pozzolanic reactivity. NS-particles act as nuclei (Kernels) to promote cement hydration. Therefore, the intensity of CSH and calcite phases increase with the presence of NS. In contrast, the peaks of anhydrous silicates and CH in case of OPC are higher than those of cements. The XRD data are in a good agreement with those of F.L and Wn. It can be concluded that, M2 is the most desirable mix than the others.

G. Differential thermal analysis

Fig. (20) represents the DTA thermograms of M2, hydrated at 1, 7 and 28 days. The results show that, the endothermic peaks corresponding to hydration products (CSH, CAH, and CASH) and calcite (CC) phase increase with time in contrast with those of CH. This is mainly due to the hydration progress of cement phases and NS-pozzolanic reaction, leading to successive consumption of lime and formation of hydration products. The impact of NS content on cement hydration can be shown from Figs. (21-23), which represent the DTA thermograms of NS-blended cement mixes comparing with the hydrated control mix at the same age. The peaks located below 200°C are due to the interlayer water of CSH, CAH and CASH. The peaks located at 295–320°C are due to the decomposition of CASH. The endothermic peak in the range 410–450°C refers to the dehydration of free Ca(OH)₂. The area of this peak decreases with NS content. Also, the results show that, the peak corresponding to CSH of OPC has lower intensity than those of OPC–NS cement mixes. This is mainly due to the pozzolanic reaction of NS with the liberated Portlandite during the hydration of β-C₂S and C₃S, leading to the production of additional CSH. The CSH peak increases with NS, % in the ascending order: M0<M3<M1<M2. It is clear that, the results of DTA are in a good harmony with those of XRD and chemical analyses.

H. Interpretation of microstructures

Based on the results of compressive strength test, it is expected that, NS behaves not only as filler to improve the internal microstructure of cement paste but also as a promoter of cement hydration and pozzolanic reaction with free CH. To verify these mechanisms, we have microscopically analyzed the hydration products of M0, M2 and M3 at 28 days (Fig. 24). It is clear that, CSH gel existed in the form of 'stand-alone' clusters, lapped and jointed together by many needle hydrates with the deposition of Ca(OH)₂ crystals, which distributed in the SEM micrograph of OPC paste. On the other side, the microstructures of NS-cement pastes revealed a pore filling with dense and compact structure. The presence of Ca(OH)₂ crystals are approximately absent, due to the pozzolanic reaction of NS with free Portlandite. Thus the number and size of CH crystals are reduced. The beneficial effect of NS results from the microstructure improvement of cementitious paste. This improvement can be interpreted as follows [49]: Suppose that NS-particles are uniformly dispersed in cement paste, and then hydrated. After the hydration begins, the hydrated products will diffuse and envelop the nano-particles (NPs) as kernels. If the NPs content and the distance between them are appropriate, the crystallization will be controlled to be a suitable state through restricting the growth of CH crystal by NPs. Moreover, the NPs located in cement paste as kernels can further promote cement hydration. This makes the cement matrix more homogeneous and compact. The increase of NPs, % than certain limit (4%) weakened the pore structure of cement paste [50, 51]. This may be attributed to that, the intermolecular distances of cement matrix decreases with increasing NS % and Ca(OH)₂ crystals cannot grow up enough, due to limited space. Therefore, the crystal quantity is decreased, leading to the decrease of crystal strengthening gel ratio. Thus the pore structure of cement matrix is looser relatively [52, 53]. Figures (25-27) represent the microstructure improvement with curing age for M0, M2 and M3 respectively. The micrographs show increase of compaction and homogeneity of the internal microstructure with curing time for all hydrated mixes. This is attributed to the continuous hydration of cement phases as well as the pozzolanic reaction of NS, leading to the formation of successive and amounts of denser hydration products, which responsible for compaction and strength properties.

IV. SUMMARY AND CONCLUSIONS

In the present work, the physico-mechanical properties and microstructure of Portland blended cements prepared from substitution of different percentages of OPC by NS up to 6.0 mass, % were studied. The water of consistency, initial and final setting times were determined for each cement paste. Also, the values of combined water, free lime, bulk density and compressive strength of hardened cement specimens were measured as a function of curing time up to 90-days. From the all findings it can be concluded that:

- The water demand increases with NS content up to 6.0 mass, %, due to the increase of surface area and decrease of crystal lattice.
- The initial and final setting times are elongated by replacement of OPC with 2.0 mass, % NS, due to the high water of consistency. As the NS content increases up to 4.0 %, the setting times are shortened, due to the formation of excessive amount of CSH, which accelerates the setting.
- The values of chemically combined water contents (Wn, %) increase with the NS content, due to the high-water demand and the pozzolanic activity of NS.
- The presence of NS tends to decrease the free lime contents.

- The bulk density and compressive strength of hardened cement mortars increases sharply with NS, up to 4 mass %, then decreases but still more than those of the control mortar. This improvement is due to that; nano-SiO₂ behaves not only as a filler to improve microstructure, but also as an activator to promote pozzolanic reaction. Both the nucleation and pozzolanic effects of NS lead to more accumulation and precipitation of hydration products in the open pores, leading to the formation of dense and compact microstructure. At high NS content (>4.0 mass, %), the NS-particles retard the hydration reaction and reduce the mechanical properties.

- The microstructural analysis of the hardened pastes reveals that, the replacement of OPC with NS resulted in a homogeneous microstructure, characterized by compact and small-sized C-S-H gel.
- The results of chemical and physico-mechanical tests are in a good agreement with each other and with those of XRD and SEM techniques.
- The results in hand show that, OPC can be advantageously replaced by 2.0-4.0 mass, % NS and this substitution is suggested to be the most effective level for producing high-performance blended cement.

V. REFERENCES

- [1] L.P. Singh, S.R. Karade, S.K. Bhattacharyya, M.M. Yousuf, S. Ahalawat "Beneficial role of nano-silica in cement based materials-A review" *Constr. Build. Mater.* 47 (2013), pp. 1069-107.
- [2] A.M. Said, M.S. Zeidan, M.T. Bassuoni, and Y. Tian, "Properties of concrete incorporating nano-silica", *Constr. Build. Mater.*; 36 (2012), pp. 838-844.
- [3] G. Quercia, P. Spiesz, G. Hüsken, H.J.H. Brouwers, "SCC modification by use of amorphous nano-silica", *Cem. Concr. Compos.* 45 (2014), pp. 69-81.
- [4] J.M. Stefanidou and I. Papayianni, "Influence of nano-SiO₂ on the Portland cement pastes", *Composites: Part B*; 43 (6) (2012), pp. 2706-2710.
- [5] H. Li, H. Xiao, J. Yuan, and J. Ou, "Microstructure of cement mortar with nano-particles", *Composites: Part B* 35, (2004), pp.185-189.
- [6] B.W. Jo, C.H. Kim, G.H. Tae, and J.B. Park, "Characteristics of cement mortar with nano-SiO₂ particles", *Constr. Build. Mater.* 21(6); (2007), 1351-1355.
- [7] L. Senff, J.A. Labrincha, M. Ferreira, D. Hotza, and W. L. Repette, "Effect of nano-silica on rheology and fresh properties of cement pastes and mortars", *Constr. Build. Mater.* 23, (2009), pp.2487-2491.
- [8] J.G.J. Olivier, J.M. Greet, and J.A.H.W. Peters, "Trends in global CO₂ emissions", 2012 report. PBL Netherlands Environmental Assessment Agency; (2012), p. 17.
- [9] G. Quercia, and H.J.H. Brouwers, "Application of nano-silica (nS) in concrete mixtures", In Gregor Fisher, Mette Geiker, Ole Hededal, Lisbeth Ottosen, Henrik Stang (Eds.), 8th fib International Ph.D. Symposium in Civil Engineering. Lyngby, June 20-23 (2010), Denmark, pp. 431-436.
- [10] M. Wilson, K.K.G. Smith, M. Simmons, and B. Raguse, "Nanotechnology-Basic Science and Emerging Technologies" Chapman & Hall/CRC; (2000).
- [11] J.K. Sobolev, et al. "Engineering of SiO₂ nano-particles for optimal performance in nano cement-based materials" Editors: Bittnar Z., Bartos P.J.M., Nemecek J., Smilauer V., and Zeman J. "Nanotechnology in Construction: Proceedings of the NICOM₃ Prague; (2009), pp. 139-48.
- [12] A. Porro et al. "Effects of nano-silica additions on cement pastes" Application of Nanotechnology in concrete Design Edited by Dhir R.K., Newlands M.D., Csetenyi L.J.; (2005), pp. 87-96.
- [13] J.F. Sanchez, and K. Sobolev, "Nanotechnology in concrete - a review", *Constr. Build. Mater.*; 24 (2010), pp.2060-71.
- [14] I. Zyganitidis, M. Stefanidou, N. Kalfagiannis, and S. Logothetidis, "Nano-mechanical characterization of cement-based pastes enriched with SiO₂ nano-particles", *Mat. Sci. Eng. B* 176 (9); (2011), pp.1580-1584.
- [15] Z.S. Metaxa, M.S. Konsta-Gdoutos, and S.P. Shah "Carbon nano-tubes Reinforced Concrete, Nanotechnology of Concrete" The Next Big Thing is Small ACI editors: Sobolev Konstantin, Mahmoud RedaTaha, SP-267-2; (2009).
- [16] M. Oltulu, and R. Sahin, "Single and combined effects of nano-SiO₂, nano-Al₂O₃ and nano-Fe₂O₃ powders on compressive strength and capillary permeability of cement mortar containing silica fume", *Mat. Sci. Eng., A* 528; (22-23) (2011), pp.7012-7019.
- [17] K. Sobolev, and M. Ferrara, "How nanotechnology can change the concrete world - Part 1", *American Ceramic Bulletin* 84 (10) (2005), pp. 14-17.
- [18] Ji. T. "Preliminary study on the water permeability and microstructure of concrete incorporating nano-SiO₂", *Cem. Concr. Res.* 35 (2005), pp. 1943-1947.
- [19] J.S. Belkowitz, and D. Armentrout, "An investigation of nano-silica in the cement hydration process", *Proceeding 2010 Concrete Sustainability Conference, National Ready Mixed Concrete Association, U.S.A.* (2010), pp.1-15.
- [20] A. Nazari, and S. Riahi, "The effects of SiO₂ nanoparticles on physical and mechanical properties of high strength compacting concrete" *Compos. Part B: Eng.* (42) (2011), pp. 570-578.
- [21] J.M. Heikal, S. Abd El-Aleem, and W.M. Morsi, "Characteristics of blended cements containing nano-silica" *HBRC Journal* (9) (2013), pp. 243-255.
- [22] W.J. Byung, H.K. Chang, and H.L. Jae, "Investigations on the Development of Powder Concrete with Nano-SiO₂ Particles", *KSCE Journal of Civil Engineering*, Vol. 11, No. 1 January (2007), pp. 37-42.
- [23] A.A. Maghsoudi, and F. Arabpour-Dahooei, "Effect of nano-scale materials in engineering properties of performance self-compacting concrete", *Proceeding of the 7th International Congress on Civil Engineering. Iran* (2007), pp. 1-11.
- [24] J.Y. Shih, T.P. Chang, and T.C. Hsiao, "Effect of nano-silica on characterization of Portland cement composite", *Mater. Sci. Eng. A-Struct.* 424 (2006), pp. 266-274.
- [25] G. Quercia, G. Hüsken, and H.J.H. Brouwers, "Water demand of amorphous nano silica and its impact on the workability of cement paste" *Cem. Concr. Res.* 42 (2012), pp. 344-357.
- [26] P. Hou, S. Kawashima, D. Kong, J. Corr David, J. Qian, and S.P. Shah, "Modification effects of colloidal nanoSiO₂ on cement hydration and its gel property", *Composites: Part B*; 45 (2013), pp. 440-448.
- [27] G. Land, D. Stephen, "The influence of nano-silica on the hydration of ordinary Portland cement" *J. Mater. Sci.* 47 (10) (2012), pp. 11-17.
- [28] J.Y. Shih, T. Chang, and T. Hsiao, "Effect of nano-silica on characterization of Portland cement composite", *Mater. Sci. Eng., A* 424, (2006), pp. 266-274.
- [29] A.N. Givi, S.A. Rashid, F.N.A. Aziz, and M.A.M. Salleh, "Experimental investigation of the size effects of SiO₂ nano-particles on the mechanical properties of binary blended concrete", *Composites: Part B* 41, (2010), pp. 673-677.

- [30] G.R. Babu, "Effect of nano-silica on properties of blended cement", *Int. J. computational engineering research*, 3 (5), (2013), pp.50-55.
- [31] AM. Said, MS. Zeidan, MT. Bassuoni, and Y. Tian, "Properties of concrete incorporating nano-silica", *Constr. Build. Mater.* (36) (2012), pp. 838-44.
- [32] S. Abd.El.Aleem, Mohamed Heikal, W.M. Morsi "Hydration characteristic, thermal expansion and microstructure of cement containing nano-silica", *Constr. Build. Mater.* ; 59 (2014), pp. 151–160.
- [33] J. J. Gaitero, I. Campillio, and A. Guerrero, "Reduction of the calcium leaching rate of cement paste by addition of silica nano-particles" *Cem. Concr. Res.*; 38 (2008), pp. 1112–1118.
- [34] F. Kontoleontos, PE. Tsakiridis, A. Marinos, V. Kaloidas, and M. Katsioti, "Influence of colloidal nano-silica on ultrafine cement hydration: physicochemical and micro-structural characterization", *Constr. Build. Mater.* ; (35) (2012), pp. 347-360.
- [35] LP. Singh, SK. Bhattacharyya, and S. Ahalawat, "Preparation of size controlled silica nanoparticles and its functional role in cementitious system" *J. Adv. Concr. Technol.*; 10 (2012), pp. 345–52.
- [36] M. Stefanidou, and I. Papayianni, "Influence of nano-SiO₂ on the Portland cement pastes Composites" Part B 43, (2012), pp. 2706–2710.
- [37] Magdy A. Abdelaziz, Saleh Abd El-Aleem and Wagih M. Menshaway "Effect of fine materials in local quarry dusts of limestone and basalt on the properties of Portland cement pastes and mortars" ,*International Journal of Engineering Research & Technology (IJERT)* Vol. 3 Issue 6, June (2014), pp.1038-1056.
- [38] ASTM Designation: C191, Standard method for normal consistency and setting of hydraulic cement, ASTM Annual Book of ASTM Standards, (2008).
- [39] M.A. Abd-El-Aziz, S. Abd.El.Aleem, and M. Heikal "Physico-chemical and mechanical characteristics of pozzolanic cement pastes and mortars hydrated at different curing temperatures" *Constr. Build. Mater.* 26, (2012), pp. 310–316.
- [40] H. El-Didamony, M. Abd-El. Eziz, and S. Abd.El.Aleem, "Hydration and durability of sulfate resisting and slag cement blends in Qaron's Lake water" *Cem. Concr. Res.*, 35; (2005), pp. 1592-1600.
- [41] H.W. Sufee, "Comprehensive studies of different blended cements and steel corrosion performance in presence of admixture", Ph.D. Thesis, Faculty of Science, Fayoum University, Fayoum, Egypt, (2007).
- [42] H.H. Assal, "Some studies on the possibility utilization of calcareous shale/clay deposits in building bricks industry", Ph. D. Thesis, faculty of science, Zagazig university, Zagazig, Egypt, (1995).
- [43] ASTM C109, "Strength test method for compressive strength of hydraulic cement mortars" (2007).
- [44] V.S. Ramachandran "Thermal Analysis, in; Handbook of analytical techniques in concrete science and technology" Ramachandran V.S. and Beaudoin J.J. Eds., Noyes publications, New Jersey. ISBN: 0-8155; (2001), PP.1473-1479.
- [45] A. William, "Concrete admixtures handbook, properties, science, and technology, crafts and Hobbies", (1995).
- [46] J. Bjornstrom, A. Martinelli, A. Matic, L. Borjesson, and I. Panas, "Accelerating effects of colloidal nano-silica for beneficial calcium-silicate-hydrate formation in cement", *Chemical Physic Letter*, 392, (2004), pp.242 – 248.
- [47] Y. Qing, Z.H. Zenan, K. Deyu. and C.H. Rongshen "Influence of nano-SiO₂ addition on properties of hardened cement paste as compared with silica fume". *Construction and Building Materials*, 21, (2007), pp. 539–545.
- [48] M. AbdEl.Aziz, S. Abd El Aleem, M. Heikal, and H. El. Didamony. "Effect of Polycarboxylate on Rice Husk Ash Pozzolanic Cement" *Sil. Ind.*, 69, 9-10; (2004), pp. 73-84.
- [49] H. Li, M. Zhang, and J. Ou. "Flexural fatigue performance of concrete containing nano particles for pavement". *Int. J. Fatigue*; 29, (2007), pp.1292–301.
- [50] X.F. Gao, Y. Lo, C.M. Tam, and C.Y. Chung. "Analysis of the infrared spectrum and microstructure of hardened cement paste" *Cem. Concr. Res.*, 29, (1999), 805-812.
- [51] W. Zhongwei, L. Huizhen, "High Performance Concrete" Beijing: China Railway Publishing Company; (1999), pp. 49–50.
- [52] W. Xin, T. Xunyan, Y. Yansheng, and Z. Yu, "Analysis on Toughening Mechanisms of Ceramic Nano-Composites" *J Ceram* 2000; 2:107–11.
- [53] W. Xijun, and Z. Mingwen, "Properties and Interfacial Microstructures for Nano-structured Materials" *Chin J Atomic Mol Phys* 1997; 2:148–52.

Table 1: Chemical oxide analysis of OPC (mass, %)

Oxides	SiO ₂	Al ₂ O ₃	Fe ₂ O ₃	CaO	MgO	SO ₃	Na ₂ O	K ₂ O	F.L	I. L	Total
mass,%	19.30	3.94	3.80	62.67	1.90	3.22	0.44	0.39	0.30	3.04	99.70

Table 2: Mineralogical composition of OPC

Compound	Abbreviation	Chemical formula	Content, %
Tri-calcium silicate	C ₃ S	3CaO.SiO ₂	66.08
Di-calcium silicate	C ₂ S	2CaO.SiO ₂	5.50
Tri-calcium aluminate	C ₃ A	3CaO.Al ₂ O ₃	4.02
Tetra-calcium aluminoferrite	C ₄ AF	4CaO.Al ₂ O ₃ .Fe ₂ O ₃	11.55

Table 3: Mix composition of blended cements, (mass, %)

Mix No.	M0	M1	M2	M3
OPC,%	100	98	96	94
N.S,%	0	2	4	6

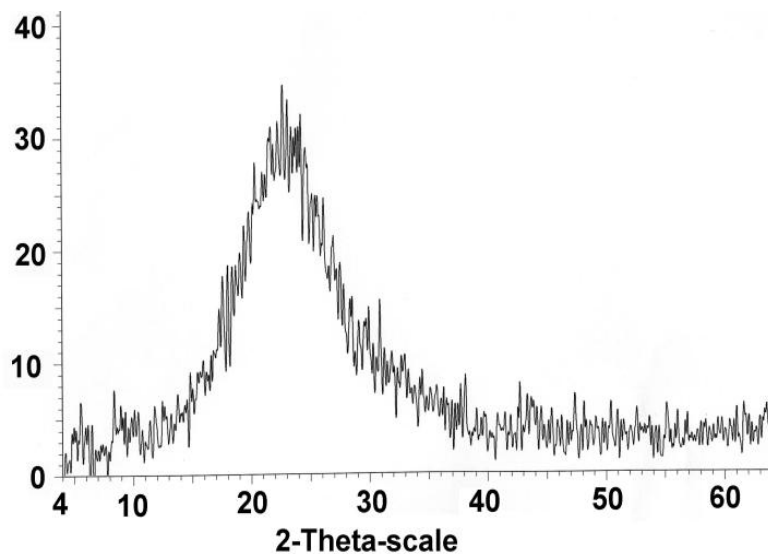


Fig.(1): XRD pattern of nano-silica (NS)

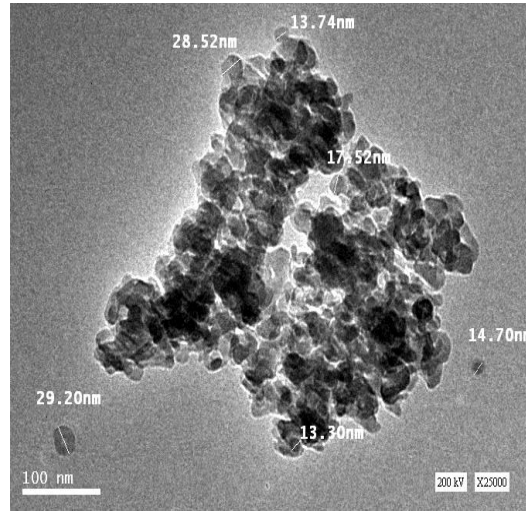
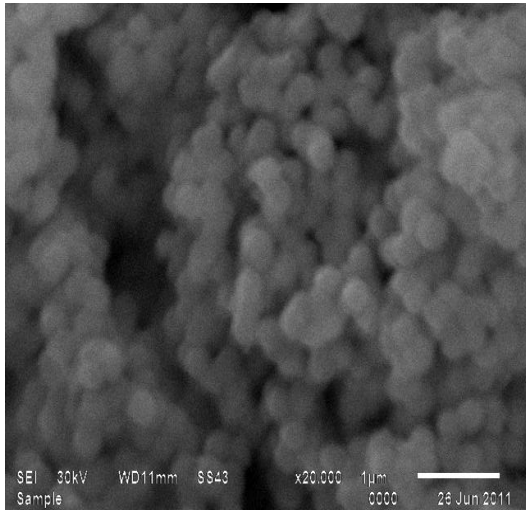


Fig. (2): SEM of nano-silica Fig. (3): TEM of nano- silica



(A)



(B)



(C)



(D)

Fig. 4 (A, B, C, D): Incubation steps of cement specimens



Fig.(5): Compressive strength machine



Fig. (6): X-ray diffractometer



Fig. (7): Scanning electron microscope

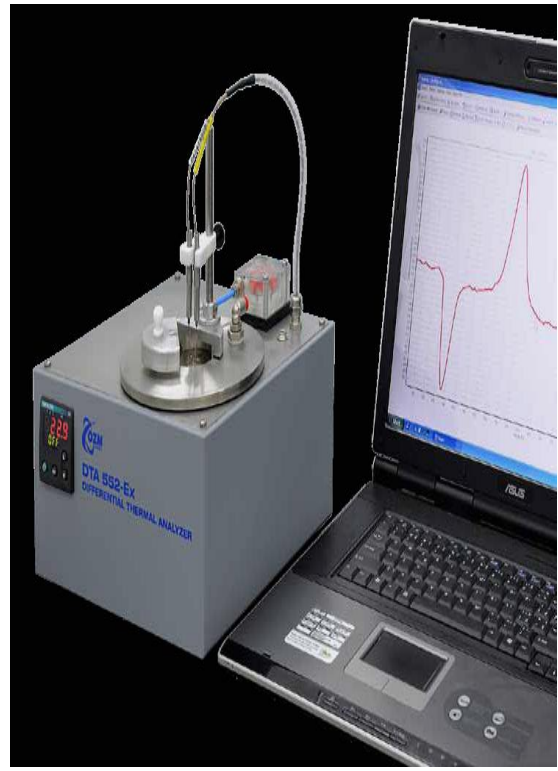


Fig. (8): Thermal analyzer

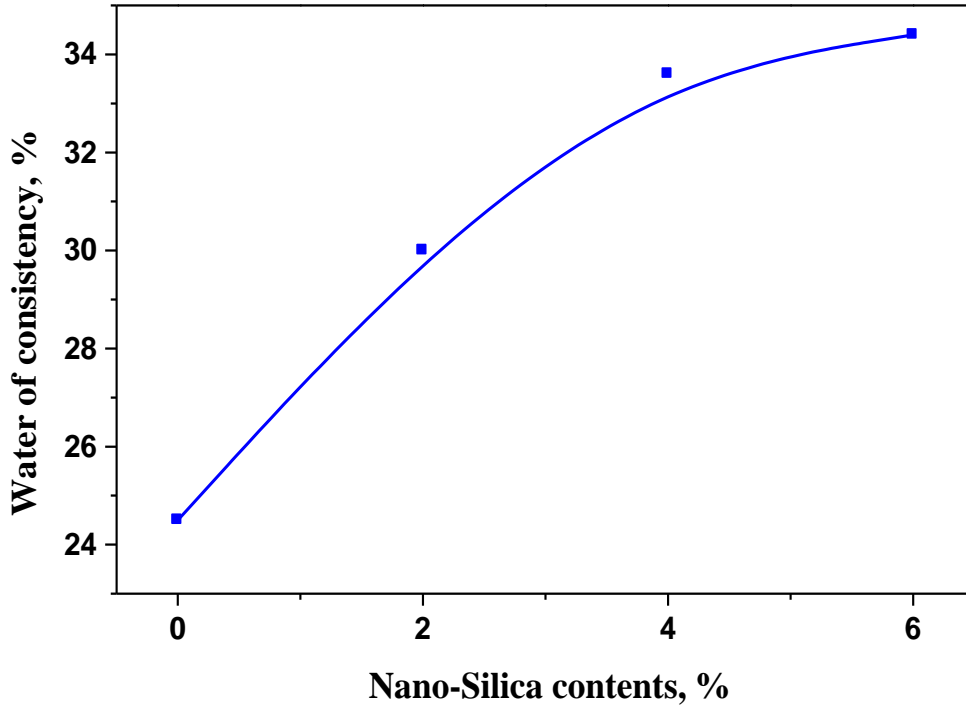


Fig. (9): Water of consistency of OPC and NS-cement pastes

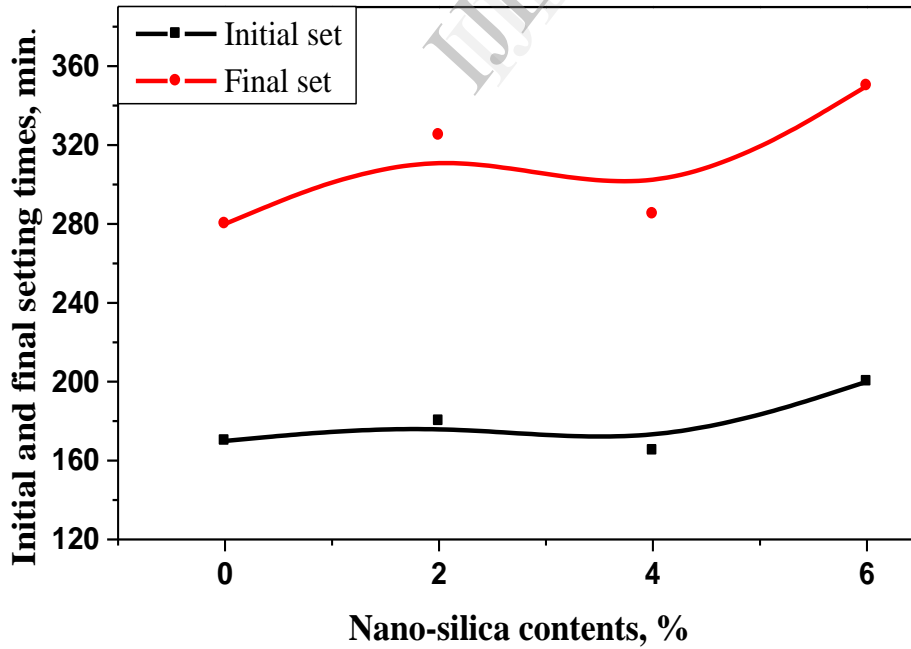


Fig. (10): Initial and final setting times of OPC and NS-cement pastes

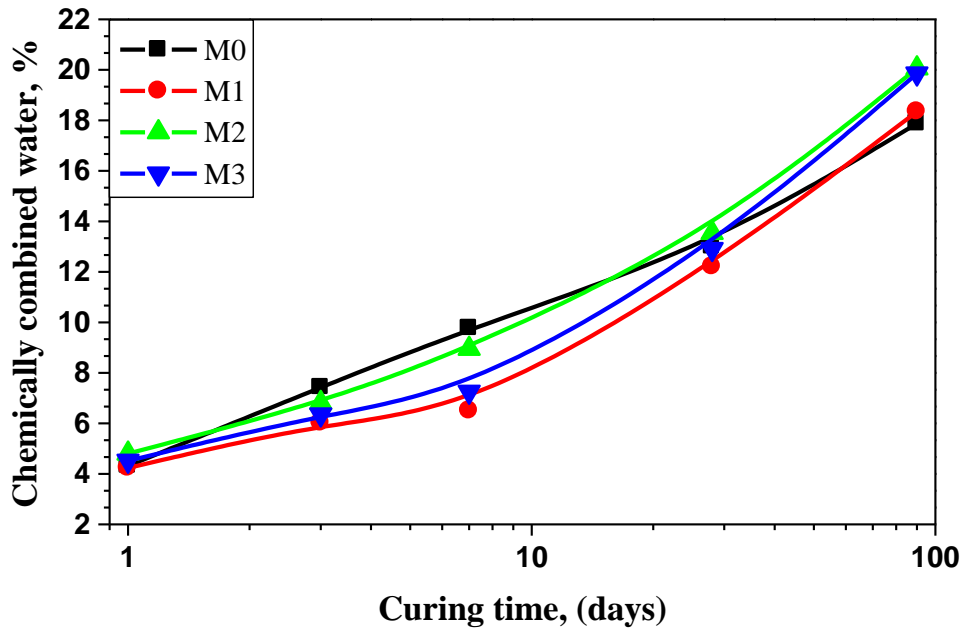


Fig.(11): Combined water contents of the hydrated OPC and NS-cement with curing time up to 90 days

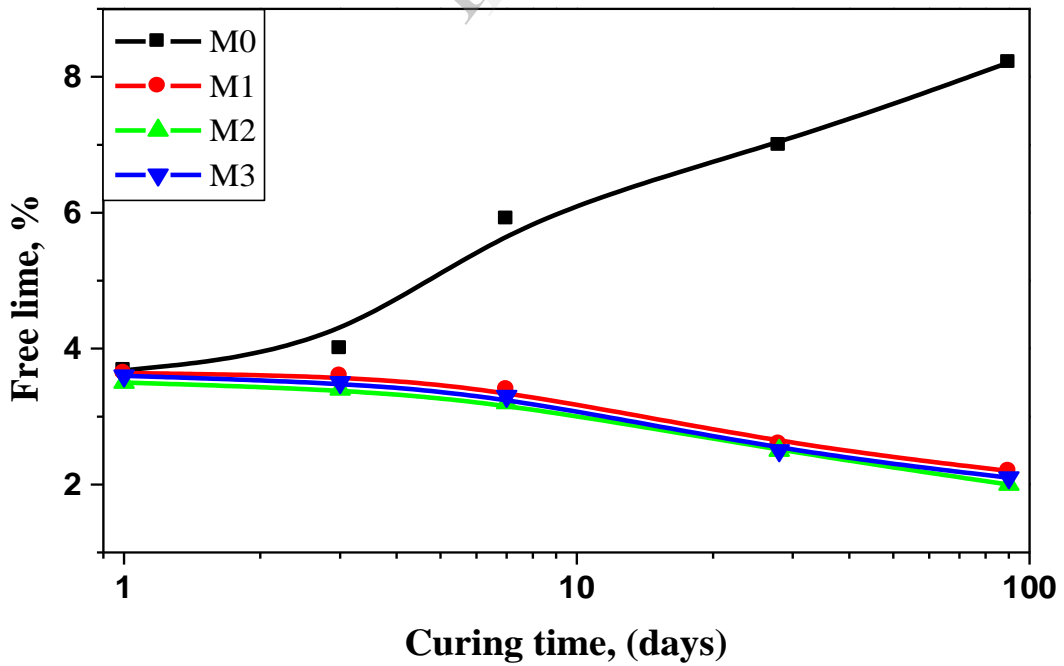


Fig. (12): Free lime contents of hydrated OPC and NS-cement pastes with curing time up to 90 days

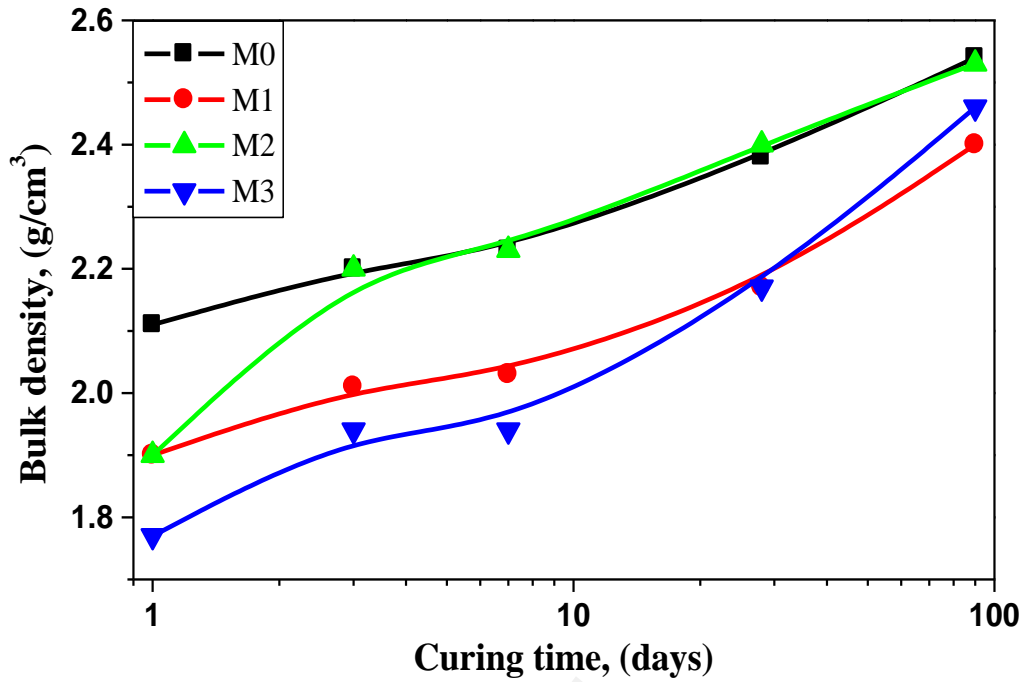


Fig. (13): Bulk density of the hardened OPC and NS-cement pastes as a function of curing time

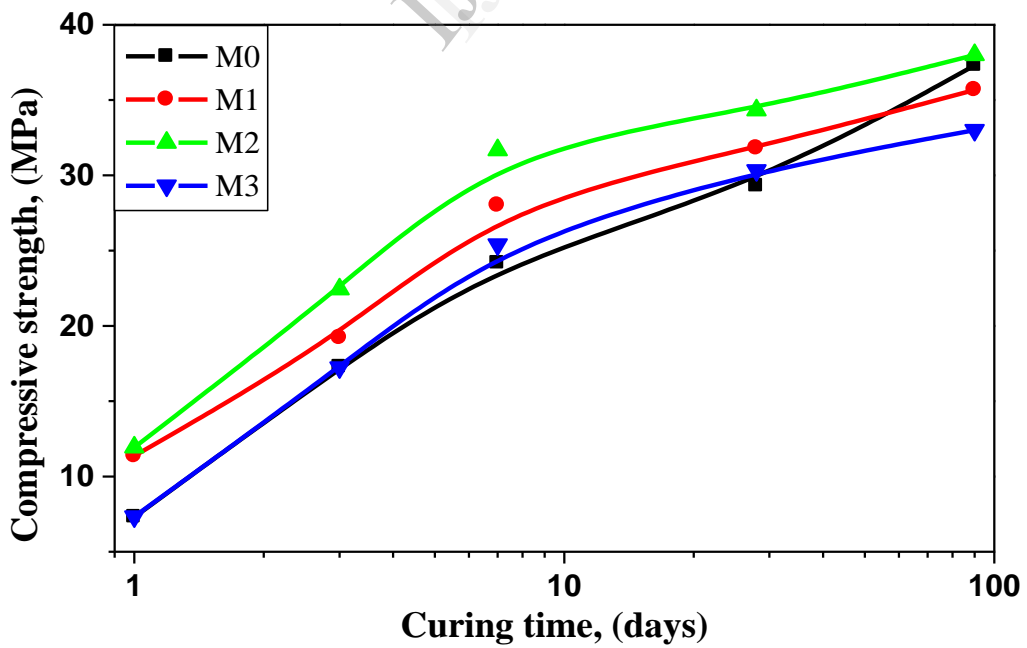


Fig. (14): Compressive strength of the hardened OPC and NS-cement mortars as a function of curing time

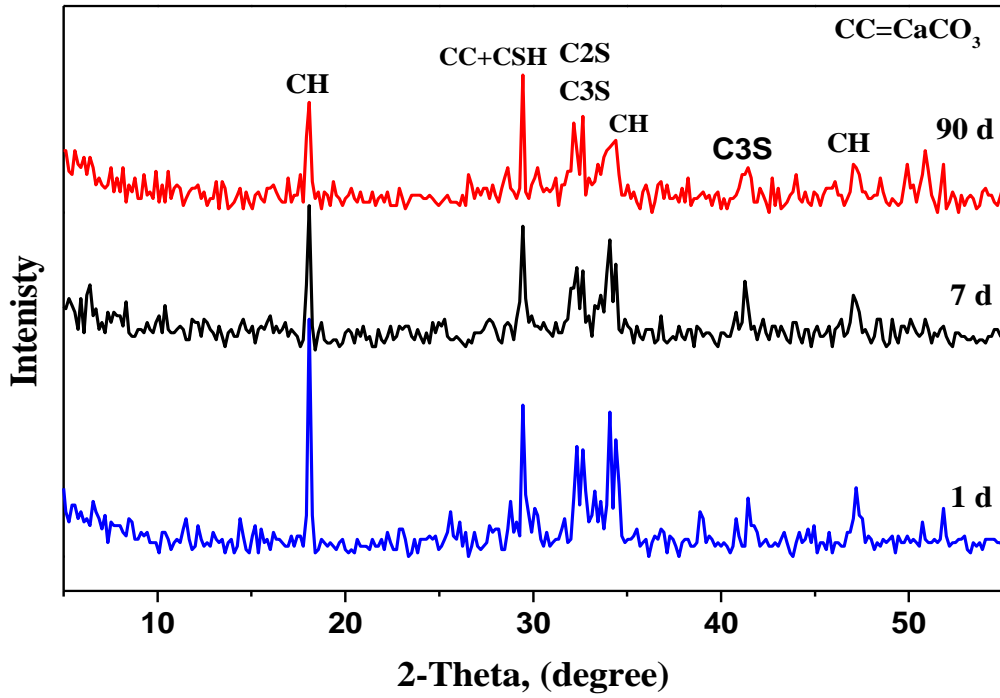


Fig. (15): XRD patterns of M2 with curing time

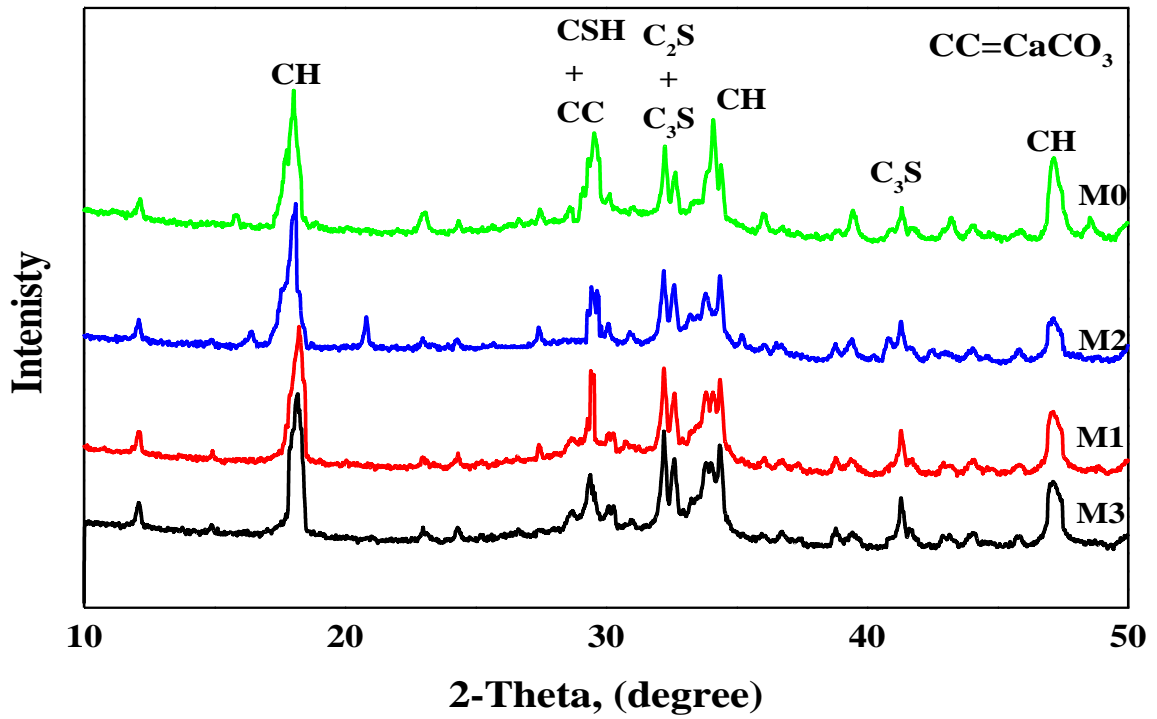


Fig. (16): XRD patterns of different mixes hydrated at 1-day

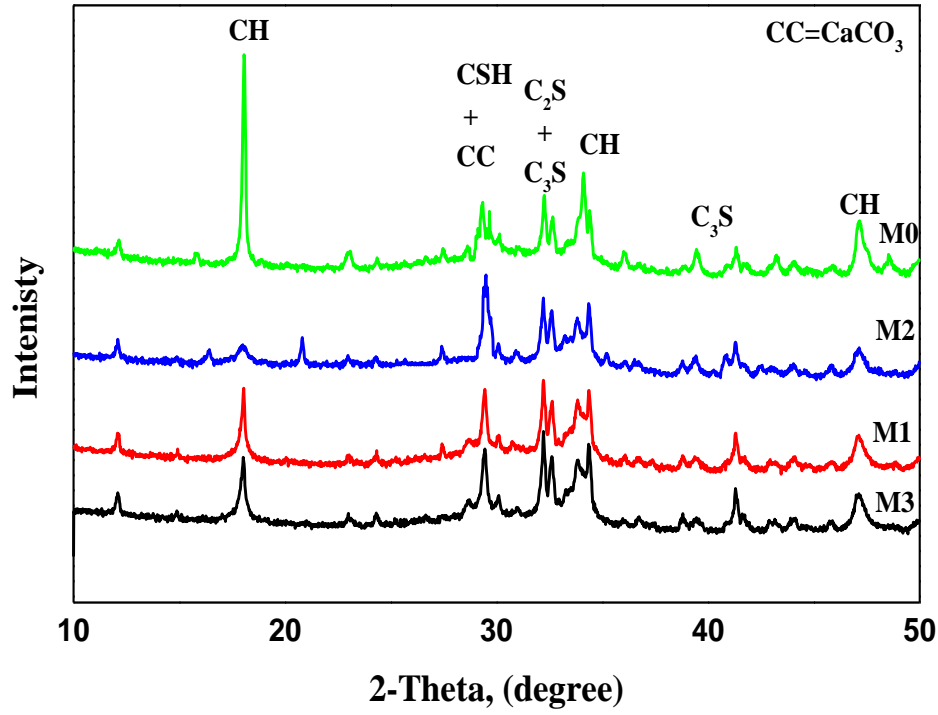


Fig. (17): XRD patterns of different mixes hydrated at 28-days

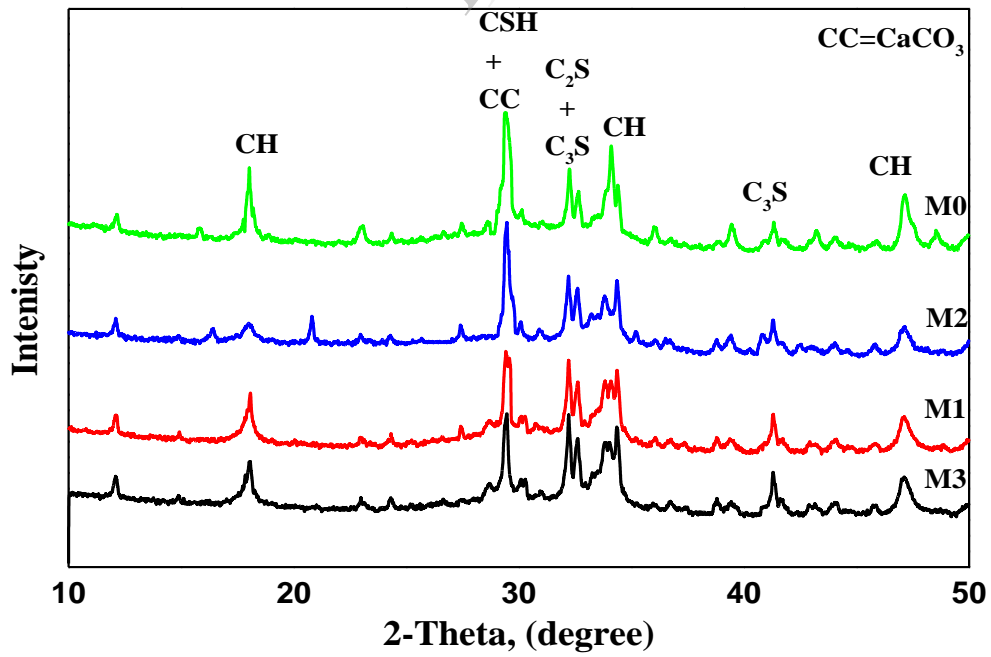


Fig. (18): XRD patterns of different mixes hydrated at 90-days

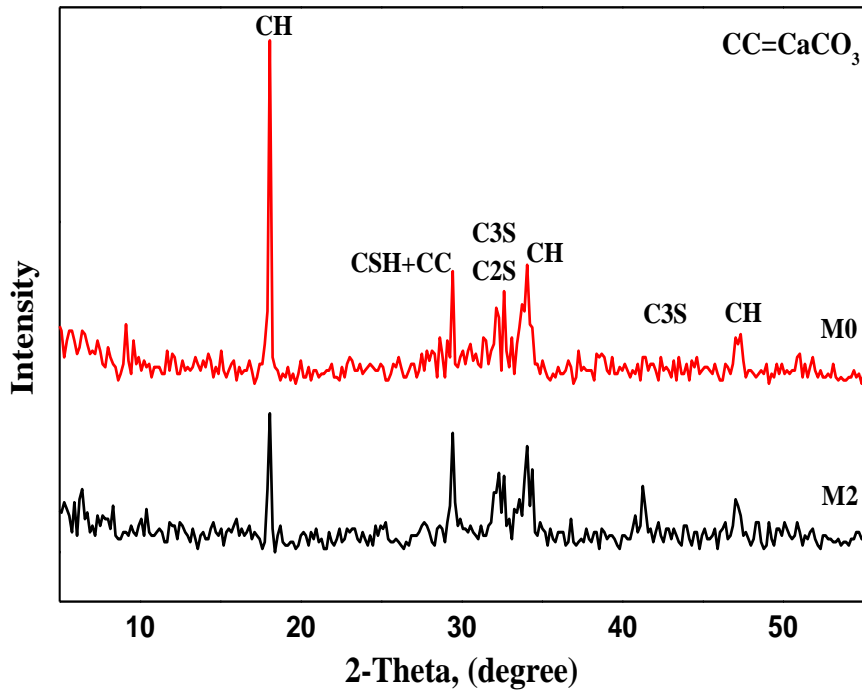


Fig. (19): XRD patterns of M0 and M2 hydrated at 7 days

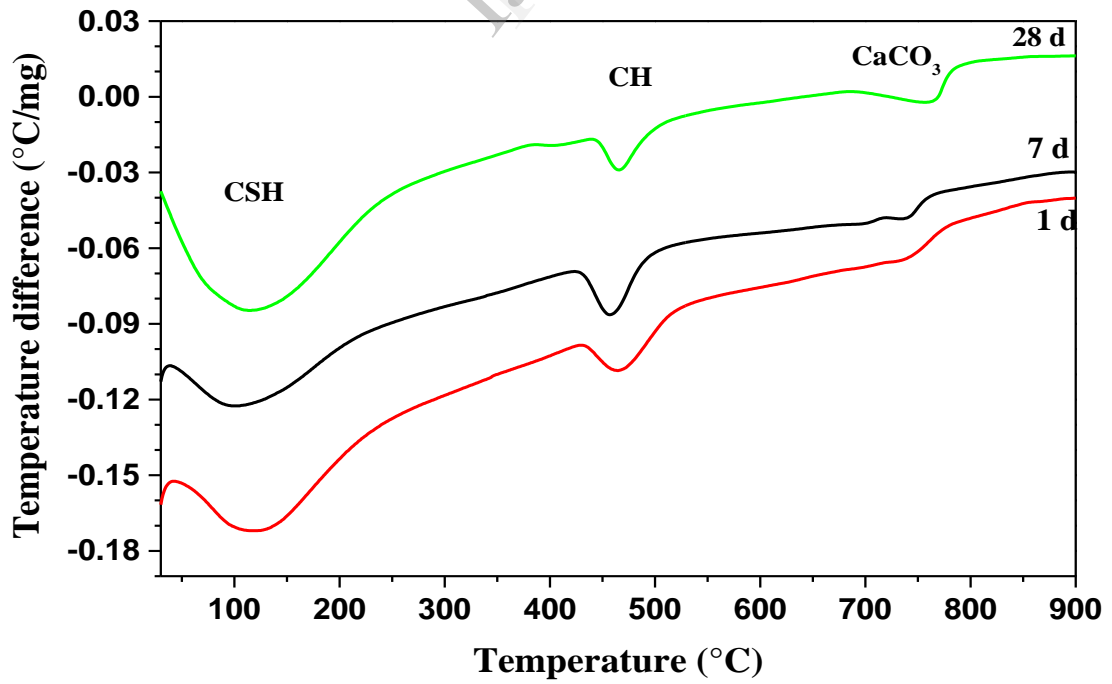


Fig. (20): DTA thermograms of (M2) as a function of curing time

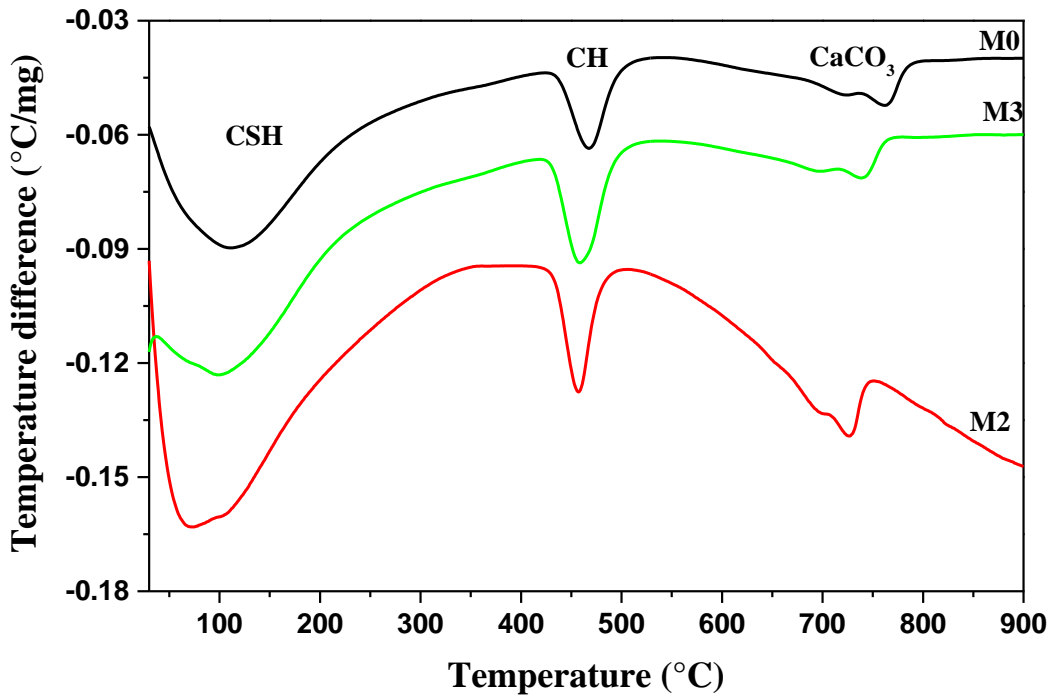


Fig. (21): DTA thermograms of different mixes hydrated at 1-day

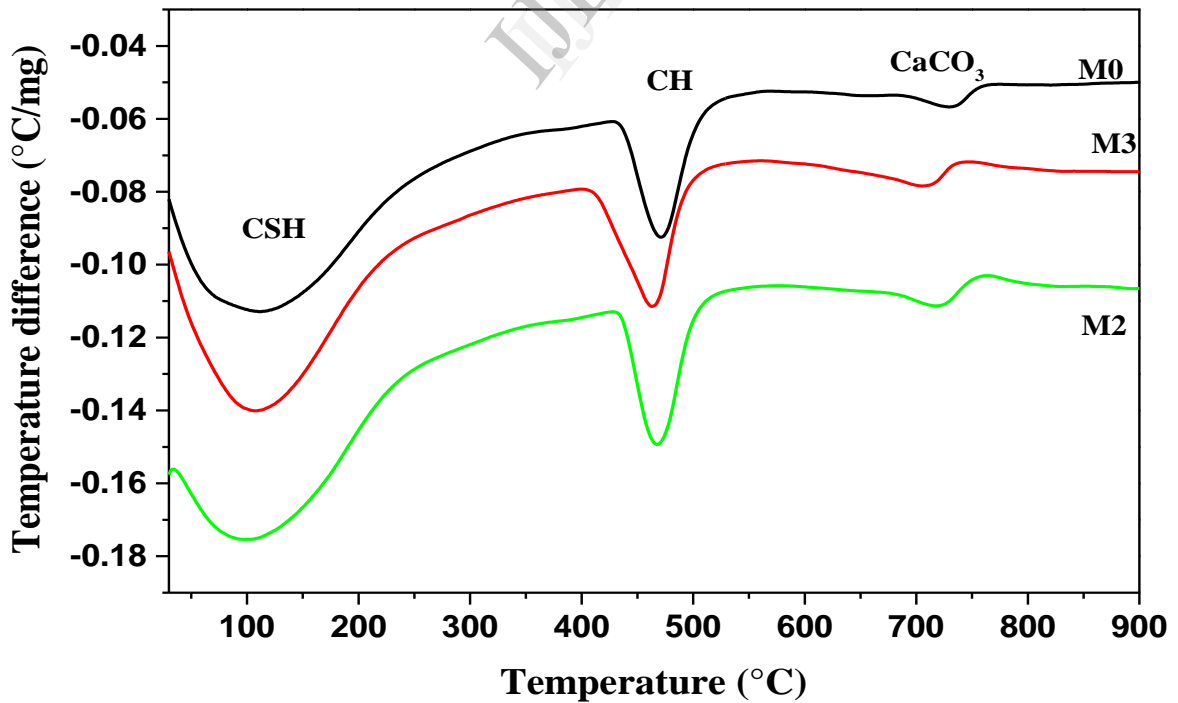


Fig. (22): DTA thermograms of different mixes hydrated at 28-days

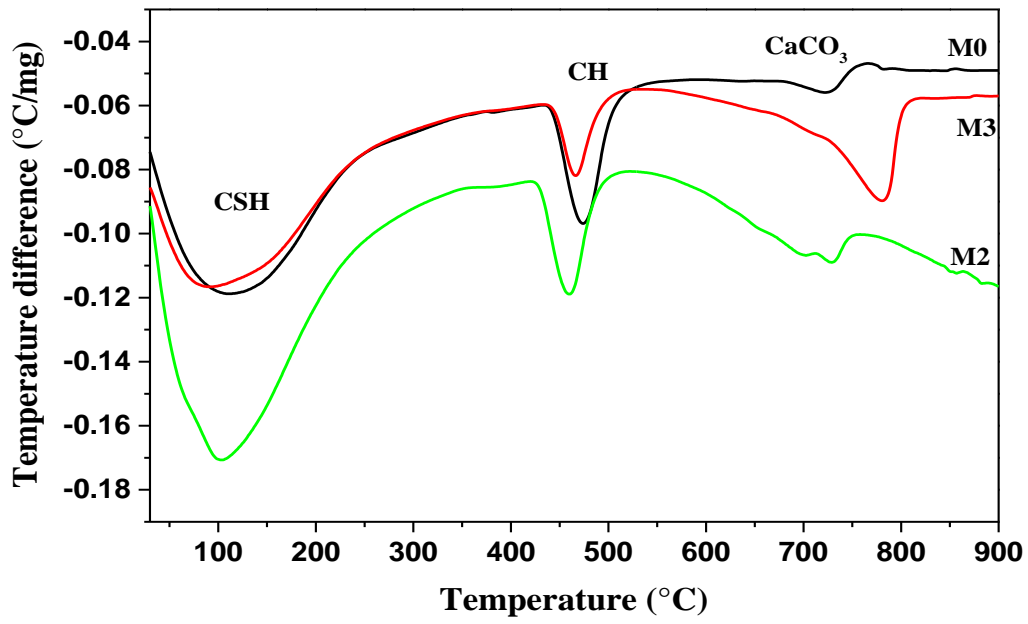


Fig. (23): DTA thermograms of different mixes hydrated at 90-days

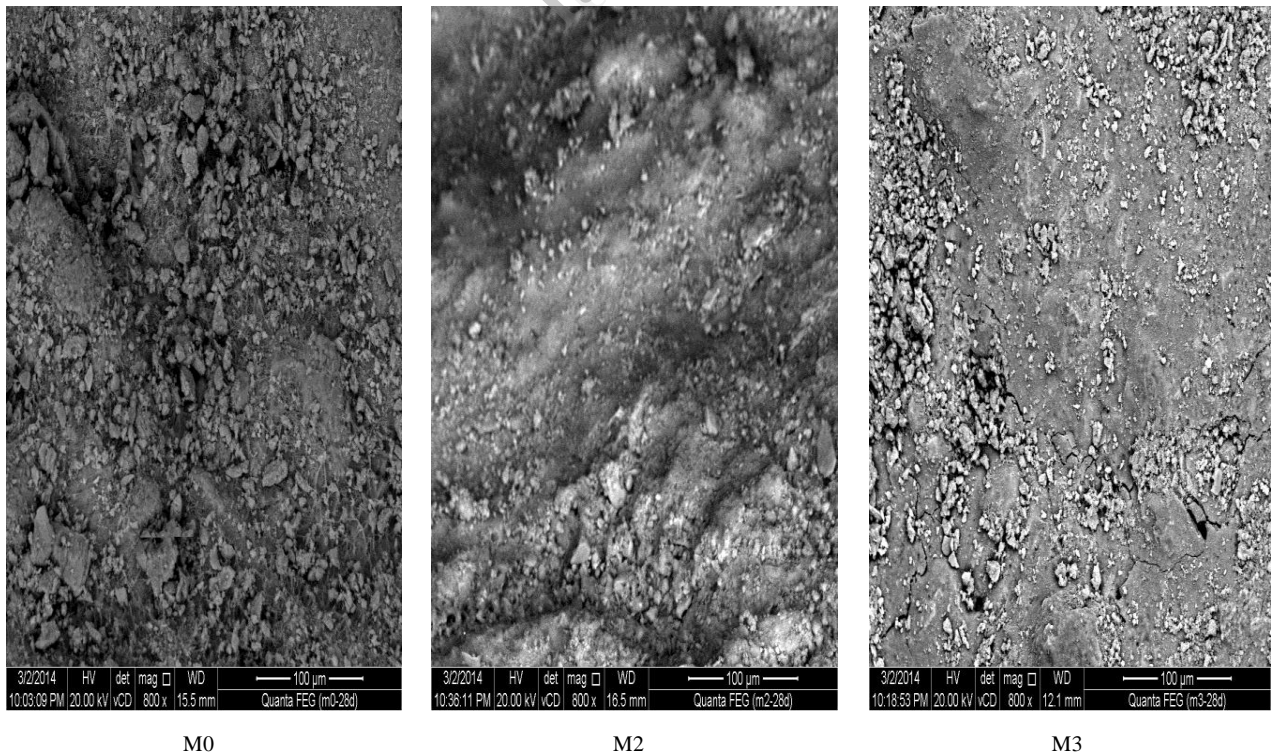
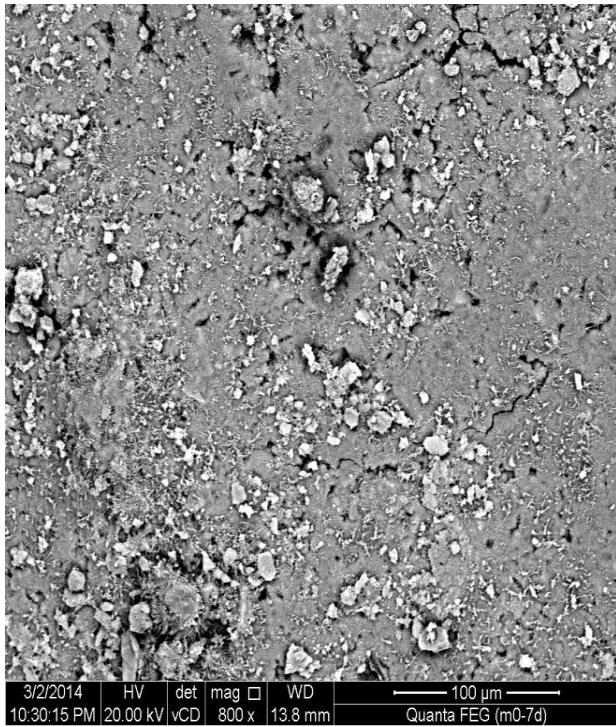
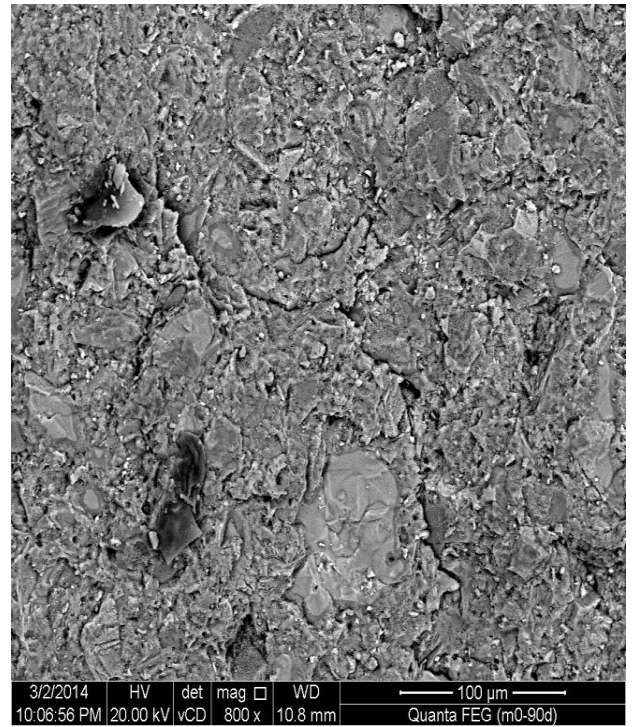


Fig. (24): SEM of M0, M2 and M3 at 28-days from left to right respectively

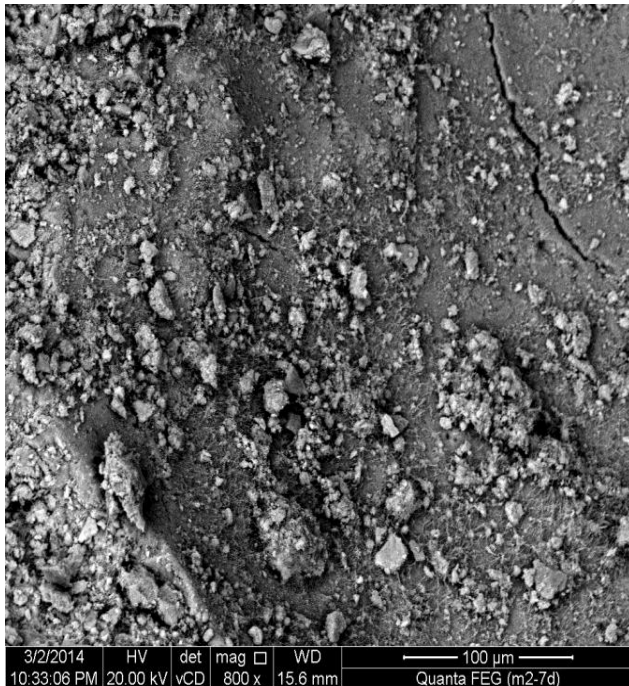


7-days

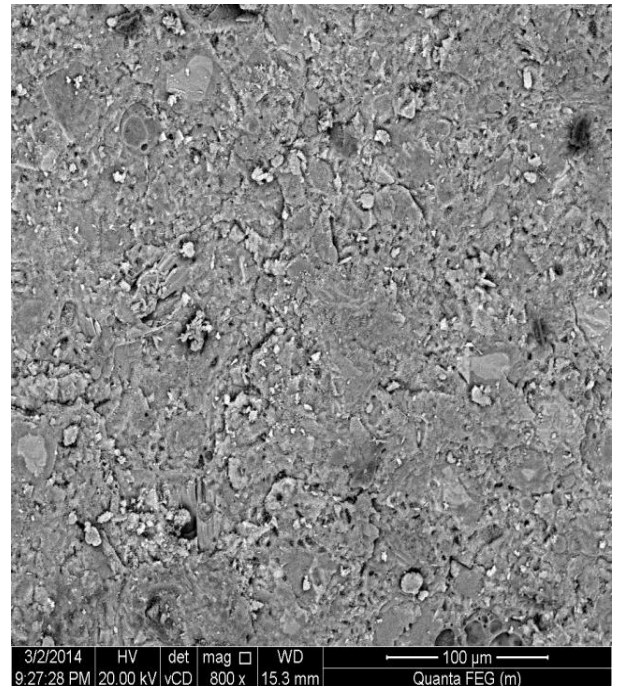


90-days

Fig. (25): SEM of M0 at 7 and 90-days from left to right respectively



7-days



90-days

Fig. (26): SEM of M2 at 7 and 90-days from left to right respectively

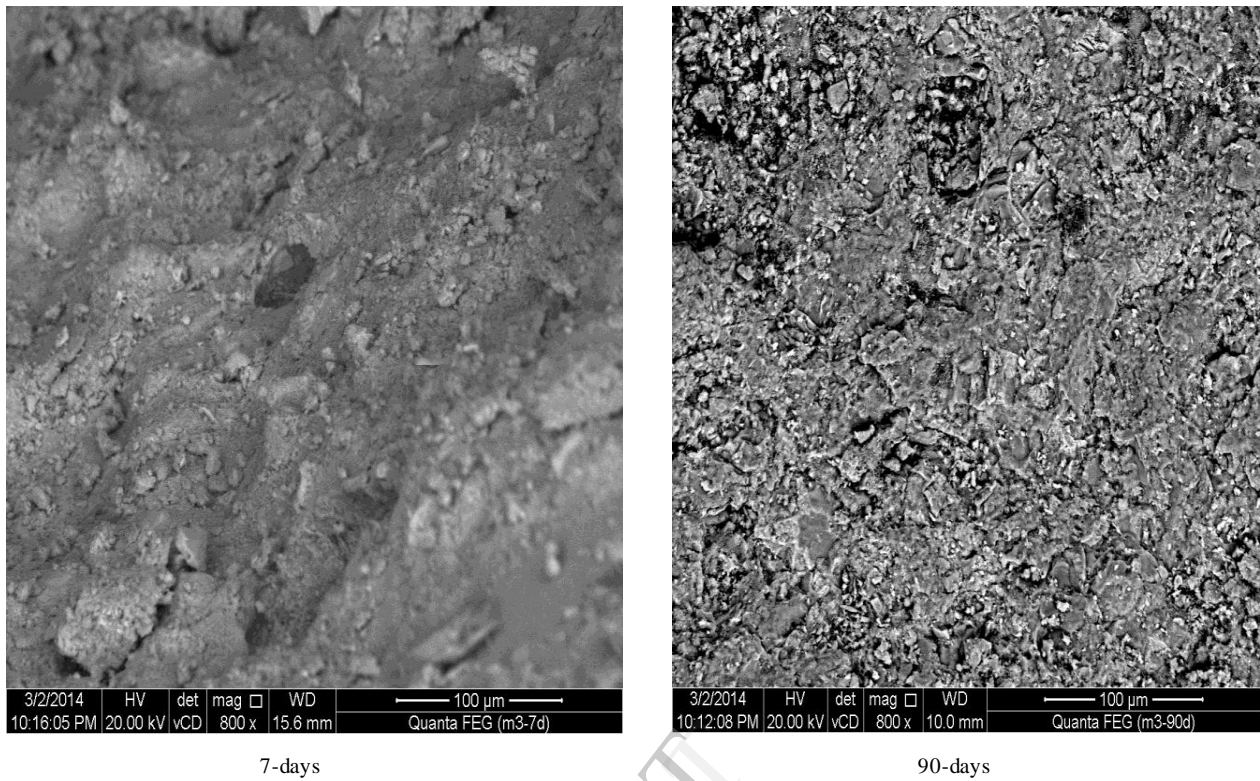


Fig. (27): SEM of M3 at 7 and 90-days from left to right respectively